

# Decellularized liver scaffolds effectively support the proliferation and differentiation of mouse fetal hepatic progenitors

Xiaojun Wang,<sup>1,2\*</sup> Jing Cui,<sup>2,3</sup> Bing-Qiang Zhang,<sup>2,3</sup> Hongyu Zhang,<sup>2,3</sup> Yang Bi,<sup>2,3</sup> Quan Kang,<sup>2,3</sup> Ning Wang,<sup>1,2</sup> Ping Bie,<sup>1</sup> Zhanyu Yang,<sup>1</sup> Huaizhi Wang,<sup>1</sup> Xiangde Liu,<sup>1</sup> Rex C. Haydon,<sup>2</sup> Hue H. Luu,<sup>2</sup> Ni Tang,<sup>2,3</sup> Jiahong Dong,<sup>1,4</sup> Tong-Chuan He<sup>2,3</sup>

<sup>1</sup>Institute of Hepatobiliary Surgery, Southwest Hospital, Third Military Medical University, Chongqing 400038, China

<sup>2</sup>Department of Surgery, Molecular Oncology Laboratory, The University of Chicago Medical Center, Chicago, Illinois 60637

<sup>3</sup>Key Laboratory of Diagnostic Medicine designated by the Chinese Ministry of Education, and the Affiliated Hospitals of Chongqing Medical University, Chongqing 400016, China

<sup>4</sup>The Hospital & Institute of Hepatobiliary Surgery, Chinese PLA General Hospital, Chinese PLA Postgraduate Medical School, Beijing 100853, China

Received 9 March 2013; revised 3 April 2013; accepted 18 April 2013

Published online 00 Month 2013 in Wiley Online Library (wileyonlinelibrary.com). DOI: 10.1002/jbm.a.34764

**Abstract:** Decellularized whole organs represent ideal scaffolds for engineering new organs and/or cell transplantation. Here, we investigate whether decellularized liver scaffolds provide cell-friendly biocompatible three-dimensional (3-D) environment to support the proliferation and differentiation of hepatic progenitor cells. Mouse liver tissues are efficiently decellularized through portal vein perfusion. Using the reversibly immortalized mouse fetal hepatic progenitor cells (iHPCs), we are able to effectively recellularize the decellularized liver scaffolds. The perfused iHPCs survive and proliferate in the 3-D scaffolds *in vitro* for 2 weeks. When the recellularized scaffolds are implanted into the kidney capsule of athymic nude mice, cell survival and proliferation of the implanted scaffolds are readily detected by whole body imaging for 10 days. Furthermore, epidermal growth factor (EGF) is shown to

significantly promote the proliferation and differentiation of the implanted iHPCs. Histologic and immunochemical analyzes indicate that iHPCs are able to proliferate and differentiate to mature hepatocytes upon EGF stimulation in the scaffolds. The recellularization of the biomaterial scaffolds is accompanied with vascularization. Taken together, these results indicate that decellularized liver scaffolds effectively support the proliferation and differentiation of iHPCs, suggesting that decellularized liver matrix may be used as ideal biocompatible scaffolds for hepatocyte transplantation. © 2013 Wiley Periodicals, Inc. *J Biomed Mater Res Part A*: 00A:000–000, 2013.

**Key Words:** cell transplantation, liver progenitor cells, immortalized progenitors, decellularized scaffolds, tissue engineering, regenerative medicine

**How to cite this article:** Wang X, Cui J, Zhang B-Q, Zhang H, Bi Y, Kang Q, Wang N, Bie P, Yang Z, Wang H, Liu X, Haydon RC, Luu HH, Tang N, Dong J, He T-C. 2013. Decellularized liver scaffolds effectively support the proliferation and differentiation of mouse fetal hepatic progenitors. *J Biomed Mater Res Part A* 2013;00: 000–000.

## INTRODUCTION

Successful organ transplantation is the ultimate treatment for end-stage organ failure.<sup>1–7</sup> However, the demand for suitable organs for transplantation far exceeds the available donor organs. Thus, there is an urgent need to develop solid organs for transplantation using tissue engineering and regenerative medicine-based strategies. The ultimate goal of tissue engineering is to reconstruct tissues or organs in order to physically and/or functionally replace damaged and injured organs. A successful tissue engineering endeavor consists of at least three essential components, including tissue-specific cells, scaffolding biomaterials and

an appropriate environment for promoting tissue formation.<sup>2–7</sup> Significant advances have been made in the development of engineered tissues, such as blood vessels, urinary bladder and trachea.<sup>2–7</sup> However, whole organ construction for large organs, such as the heart, lung, liver, and kidney, requires immediate access to the blood supply after transplantation, which requires extensive vascular networks for nutrient and gas exchange in order to obtain nutrients and oxygen.<sup>1</sup>

Whole organ decellularization represents an ideal choice for the fabrication of scaffolds for engineering new organs because the scaffolds should consist of naturally derived

\*Recipient of the predoctorate fellowship from the China Scholarship Council.

**Correspondence to:** T.-C. He; e-mail: tche@uchicago.edu and J. Dong; e-mail: dongjh301@163.com

Contract grant sponsor: National Institutes of Health (to TCH, RCH, and HHL)

Contract grant sponsor: Natural Science Foundation of China (NSFC); contract grant numbers: #81100309 (to YB) and #30972586 and #31171307 (to NT)

Contract grant sponsor: Key National S & T Program; contract grant numbers: #2013ZX10002002-005-003 and #2012ZX10002005-003-002 (to NT)

extracellular matrix (ECM) and thus maintain tissue micro-architecture, including intact vascular networks ready to integrate into the recipient's circulatory system. A significant advancement in the field of bioscaffold design is the utilization of decellularized tissue as the three-dimensional (3-D) scaffold in tissue engineering strategies. The decellularized tissues, which have no intact cells and nuclei but remain collagen, elastic fibers and intact ECM network, have been proved as an effective barrier to penetration of the scaffold by seeded cells.<sup>8-11</sup> The seeded cells can be mature cells or fetal cells.<sup>12</sup> The ECM consists of a complex mixture of functional and structural molecules, which are usually arranged in a unique, tissue-specific, 3-D ultrastructure and are ideally suited to the tissue or organ from which the ECM is harvested. Because the ECM is produced by the resident cell populations, it is logical that the specific composition and ultrastructural organization of the component molecules will vary depending on the source tissue/organ from which the ECM scaffold is prepared. Accordingly, the potential importance of organ specificity with regard to the source of ECM may be considered as a template for organ restoration. For example, ECM harvested from liver tissue may be the preferred ECM substrate for hepatocytes.<sup>1,2</sup>

Hepatocyte transplantation has been considered as an attractive alternative to liver transplantation for a variety of liver diseases.<sup>2</sup> Clinical application of hepatocyte transplantation has been limited by good quality donor livers for the isolation of cells. Although the recently discovered technologies for reprogramming of postnatal cells into pluripotent stem cells may offer a promising approach toward the generation of patient-specific autologous cells, many issues regarding the safety and efficacy need to be answered before these cells can be applied in clinical trials.

In this study, we investigate whether the decellularized liver matrix scaffolds can efficiently support the survival and proliferation of hepatic progenitor cells both *in vitro* and *in vivo*. We demonstrate that mouse liver tissues are efficiently decellularized through a simplified portal vein perfusion procedure. Using the reversibly immortalized mouse fetal hepatic progenitor cells (iHPCs), we are able to effectively recellularize the decellularized liver scaffolds. The perfused iHPCs can survive and proliferate in the 3-D scaffolds *in vitro* for up to 2 weeks. When the recellularized scaffolds are implanted into the kidney capsule of athymic nude mice, the cell survival, and proliferation of the implanted scaffolds are readily detected by whole body imaging for up to 10 days. Furthermore, epidermal growth factor (EGF) is shown to significantly promote the survival and proliferation of the implanted iHPCs. The histologic and immunochemical analyses indicate that the iHPCs are able to proliferate and differentiate to mature hepatocytes upon EGF stimulation in the scaffolds. Interestingly, the recellularization of the biomaterial scaffolds was accompanied with vascularization within the scaffolds. Thus, these results demonstrate that decellularized liver scaffolds may effectively support the proliferation and differentiation of iHPCs, suggesting that the decellularized matrix may be ideal scaffolds for hepatocyte transplantation.

## MATERIALS AND METHODS

### Cell culture and chemicals

HEK-293 cells were purchased from ATCC (Manassas, VA) and were maintained in complete Dulbecco's Modified Eagle's Medium (DMEM) containing 10% fetal bovine serum (FBS, Invitrogen), 100 units/mL of penicillin and 100 µg/mL of streptomycin at 37°C in 5% CO<sub>2</sub>.<sup>13,14</sup> The retinoic acids were purchased from Enzo Life Sciences (NY) and dissolved in dimethyl sulfoxide (DMSO). Recombinant human EGF (rhEGF) was purchased from Sigma-Aldrich (St. Louis, MO). Unless indicated otherwise, all chemicals were purchased Fisher Scientific (Pittsburgh, PA).

### Construction and generation of recombinant adenoviruses expressing EGF, β-catenin, or green fluorescent protein

Recombinant adenoviruses were generated using the AdEasy technology as described.<sup>15-19</sup> The coding regions of human EGF and human oncogenic mutant β-catenin were polymerase chain reaction (PCR) amplified and cloned into an adenoviral shuttle vector, and subsequently used to generate recombinant adenoviruses in HEK-293 cells. The resulting adenoviruses were designated as Ad-EGF or Adβ-catenin, both of which also express green fluorescent protein (GFP). Analogous adenovirus expressing only GFP (AdGFP) was used as controls.<sup>14,16,19-22</sup>

### Isolation and iHPCs

All animal experiments were performed by following the NIH guidelines approved by the Institutional Animal Care and Use Committee. E13.5-E14.5 embryos were obtained from timed pregnancy of CD1 female mice (Harlan Laboratories, IN). The fetal liver cells were isolated as described previously.<sup>23-25</sup> Briefly, the fetal liver tissues were dissected, rinsed with sterile ice-cold PBS, minced into small pieces, and incubated in 0.25% trypsin/1 mM ethylenediaminetetraacetic acid with gentle agitations at 37°C for 15 min. The digestion was terminated by adding 10% FBS DMEM. Cell debris/undigested tissue bits were removed by passing the mix through 100 µm cell filter strainers. Cells were seeded onto 100 mm cell culture dishes precoated with type I collagen, and incubated at 37°C and 5% CO<sub>2</sub>. Nonadherent cells were removed at 24 h. Once reaching approximately 90% confluence, cell were passaged for making immortalized cells.

For making iHPCs, a retroviral vector SSR #69 expressing SV40 large T antigen flanked with loxP sites was used.<sup>23,24,26-28</sup> Retrovirus expressing SV40 large T antigen was first packaged by cotransfecting SSR #69 and the packaging vector pCLAmpho into HEK-293 cells. The filtered viral supernatants were used to infect the primary fetal hepatocytes. The stable and immortalized cells, designated as iHPCs, were selected in the presence of 0.3 mg/mL hygromycin B (Invitrogen) for 7-10 days, as reported previously.<sup>23-25,27,28</sup>

### Construction of albumin promoter-driven Gaussia luciferase (Alb-GLuc) reporter and reporter assays

A 2.5-kb genomic DNA fragment containing the mouse albumin (Alb) gene promoter was PCR amplified and subcloned

into a homemade pSEB-GLuc retroviral vector to drive expression of Gaussia luciferase (pSEB-Alb-GLuc) as described.<sup>23,24</sup> The constructed reporter was used for transient reporter assays. Authenticity of the PCR amplified fragments was verified by DNA sequencing.

For reporter assays, subconfluent iHPCs were first transfected in 25 cm<sup>2</sup> flasks with pSEB-Alb-GLuc using LipofectAMINE (Invitrogen). At 16h post-transfection, cells were replated to 24-well plates and stimulated with rhEGF (0, 0.1, or 0.5 ng), infected with AdGFP and Ad $\beta$ -catenin, or treated with DMSO, 9-cis retinoic acid (RA, 0.5  $\mu$ M) or dexamethasone (Dex, 0.1  $\mu$ M). Culture media were collected for Gaussia luciferase assays at day 3 (for Dex, RA and  $\beta$ -catenin) or days 1 and 4 (for rhEGF), using the Gaussia Luciferase Assay Kit (New England Biolabs). All assay conditions were performed in triplicate. Reporter activity was expressed as mean  $\pm$  standard deviation.

### Generation of decellularized liver scaffolds

Male balb/c mice (25–30 g; Jackson Laboratory) were used for liver procurement. Briefly, the animals were first anesthetized with by intraperitoneal (i.p.) injections of ketamine and xylazine. The incision was made in the upper abdomen to expose the liver. A 24-gauge catheter (Terumo Medical Corporation, Elkton, MD) was cannulated into the portal vein. Blood clotting was prevented by slowly injecting 50 mL of sterile PBS (containing 12.5 U/mL heparin) into portal vein through the catheter while leaving the inferior vena cava open as an outlet flow. The perfused liver was then removed from the animal and rinsed with PBS containing 100 units/mL penicillin and 100  $\mu$ g/mL streptomycin. The excised liver tissues were transferred to 100 mm cell culture dishes and perfused for 2 h with 1% sodium dodecyl sulfate (SDS) solution, followed by 30 min perfusion with 1% Triton-X 100, both at room temperature with a perfusion rate of 5 mL/min. The decellularized liver scaffolds were perfused and washed with sterile PBS to remove any residual detergents for 3 h.

### Assessment of decellularization using DNA content analysis

The decellularized liver samples (approximately 25–30 mg) and control liver samples were minced into small pieces and digested with alkaline lysis buffer at 85°C for 20 min or until no visible materials remained. The digested mixtures were subjected to phenol–chloroform extractions and ethanol precipitation. The DNA concentrations were determined by using the PicoGreen DNA assay kit (Invitrogen). Total DNA content for each sample (ng/mg tissue) was calculated.

### Recellularization of the liver scaffolds for *in vitro* 3-D culture

The decellularized liver scaffolds were thoroughly perfused with sterile PBS to remove any residual detergents and chemicals. The scaffolds were then placed in 100 mm cell culture dishes and perfused with 5 mL of the completed DMEM (containing 10% FBS) through the catheter connected with the portal vein. Subconfluent iHPCs were

infected with AdGFP for 24 h, collected, and perfused into the decellularized liver scaffolds (10<sup>67</sup> cells/scaffold). The recellularized scaffolds were cultured in 5% CO<sub>2</sub> at 37°C for up to 14 days.

### Renal capsule grafting assay of iHPCs in a mouse model

Male athymic nude mice (25–30 g, Harlan Laboratories, IN) were used as transplant recipients. Subconfluent iHPC cells tagged with firefly luciferase (iHPC-FLuc) were transduced with AdGFP or Ad-EGF for 24 h, collected, and perfused into the decellularized liver scaffolds (10<sup>67</sup> cells/scaffold). The recellularized scaffolds were cultured for another 24 h to let the cells adhere, then gently cut into 0.5 cm<sup>3</sup> pieces, and implanted into the left kidney capsule of athymic nude mice. Scaffolds without recellularization were also performed as negative controls. The animals were not restricted to any activities for up to 10 days.

### Xenogen bioluminescence imaging analysis

Bioluminescence imaging was performed at the indicated time points. Briefly, mice were anesthetized with isoflurane attached to a nosecone mask within Xenogen IVIS 200 imaging system as described.<sup>13,29–33</sup> Mice were injected (i.p.) with D-Luciferin sodium salt (Gold BioTechnology) at 100 mg/kg in 0.1 mL PBS. The pseudoinages were obtained by superimposing the emitted light over the gray-scale photographs of the mice. Quantitative analysis was done with Xenogen's Living Image software.

### Histologic evaluation, trichrome staining, and immunohistochemical staining

The scaffolds from *in vitro* or *in vivo* studies were first fixed in 10% formalin and subjected to frozen sectioning. Sections were routinely stained with hematoxylin and eosin (H&E). Trichrome staining was performed on the decellularized liver scaffolds as described.<sup>18,28,34–37</sup> Anti-GFP immunohistochemical staining (Clontech) was performed to reaffirm the recellularization. Immunohistochemical staining was also performed using anti-mouse albumin (Alb, Santa Cruz) and anti-CD31 (Abcam, MA) were also performed as described previously.<sup>29,31,38,39</sup>

### Statistical analysis

The Prism 5 software and Microsoft Excel were used for statistical analysis. Differences between samples were analyzed by using the two-tailed Student *t* test. A *p*-value <0.05 was considered statistically significant.

## RESULTS

### Decellularized tissue scaffolds can be efficiently prepared from mouse livers using a simplified perfusion protocol

In order to prepare decellularized liver scaffolds, we used young adult male balb/c mice. While the animals were under anesthesia, mouse livers were exposed and perfused with anticoagulation heparin-containing PBS through the portal vein [Fig. 1(A), panels a and b]. The perfused liver was then removed from the animal and rinsed with

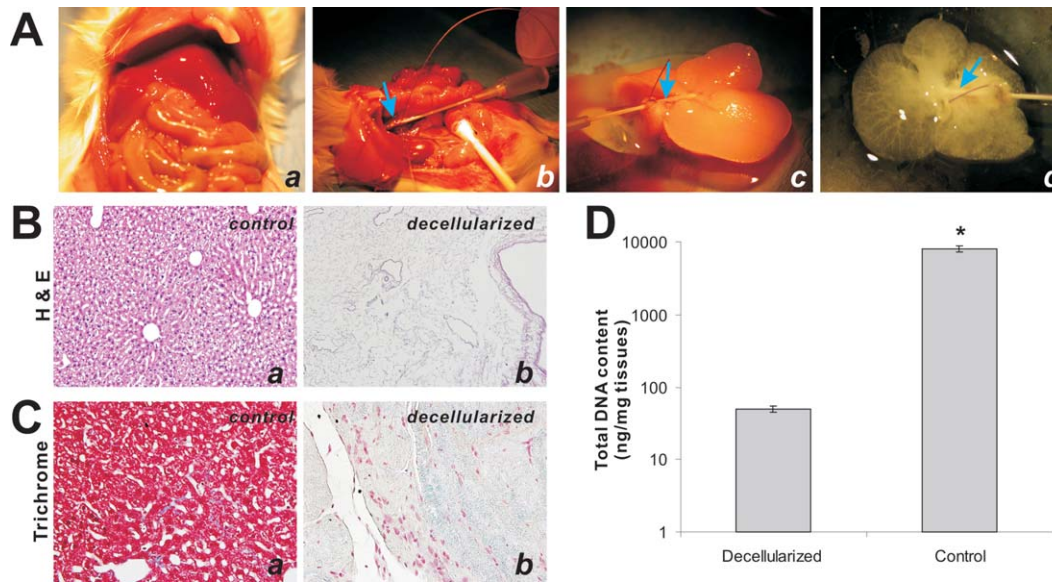


**FIGURE 1.** Generation of decellularized tissue scaffolds from mouse livers. **A**, The key steps for decellularizing mouse livers involve in (a) exposing the mouse abdomen, (b) identifying the portal vein (arrows) and inserting the catheter into the portal vein, (c) removing the liver out of abdominal cavity and perfusing the livers with 1% SDS and 1% Triton X-100, and (d) obtaining the decellularized livers after  $\times 1$  PBS perfusion. **B**, H&E staining of control (uncellularized, a) and decellularized livers (b). **C**, Trichrome staining of control (a) and decellularized liver tissues (b). Representative results are shown. **D**, Quantitative determination of the total DNA content of the control and decellularized liver tissues ( $n=5$ ). [Color figure can be viewed in the online issue, which is available at [wileyonlinelibrary.com](http://wileyonlinelibrary.com).]

antibiotics-containing PBS [Fig. 1(A), panel c], followed by perfusion with 1% Triton-X 100. The decellularized liver scaffolds were perfused and washed with sterile PBS to remove any residual detergents [Fig. 1(A), panel d]. The complete protocol for decellularization usually lasted about 4 h.

The quality of the decellularized liver scaffolds was first examined by H&E staining. Compared with the unprocessed liver tissues [Fig. 1(B), panel a], decellularized liver tissues have no identifiable cells [Fig. 1(B), panel b], indicating the decellularization was efficient and thorough. The decellularization was further confirmed by using Masson's trichrome staining. Compared with the control liver tissues [Fig. 1(C), panel a], the red-staining cytoplasm almost completely disappeared in the decellularized liver scaffolds [Fig. 1(C), panel b]. Furthermore, we determined the total DNA contents in the control livers and the decellularized scaffolds and found that the total DNA content for the decellularized liver scaffolds was about 0.6% of that for the control unprocessed liver tissues [Fig. 1(D)]. Thus, taking these results together we have demonstrated that our decellularization protocol is efficient to remove the cellular components from mouse liver tissues.

#### The decellularized liver scaffolds are efficiently recellularized with the iHPCs in 3-D culture *in vitro*

To test if the decellularized scaffolds can support the proliferation and growth of hepatocytes, we first sought to isolate and establish the iHPCs from mouse E13.5-E14.5 embryos. The fetal liver cells were isolated as described previously.<sup>23-25</sup> For making iHPCs, the retroviral vector SSR #69 expressing SV40 large T antigen flanked with loxP sites

[Fig. 2(A)] was used.<sup>23,24,26-28</sup> The stable and immortalized iHPCs were selected in the presence of hygromycin B, as described previously.<sup>23-25,27,28</sup> When seeded at the same density, the immortalized cells grew at a much faster rate than that of the primary cell's [Fig. 2(B)].

We further analyze the differentiation potential of iHPCs using the liver-specific albumin-driven Gaussia luciferase reporter (Alb-GLuc) as described previously<sup>23-25</sup> [Fig. 2(C)]. Consistent with our previously reported findings,<sup>23</sup> Dex and retinoic acid were shown to induce Alb-GLuc activity [Fig. 2(D), panel a]. When the iHPCs were transduced with adenovirus expressing the oncogenic mutant form of human  $\beta$ -catenin, Alb-GLuc activity was significantly induced [Fig. 2(D), panel a], consistent with our previously reported important roles of Wnt signaling in hepatic differentiation.<sup>24</sup> Furthermore, the rhEGF was also shown to effectively induce Alb-GLuc activity [Fig. 2(D), panel b]. These results indicate that the iHPCs have long-term proliferative activity and can differentiate hepatocyte-like cells when stimulated with proper differentiation cues.

Using the iHPCs, we sought to test whether hepatic progenitor cells would survive and propagate in the 3-D culture using the decellularized liver scaffolds. The iHPCs were first transduced with AdGFP and then perfused into the decellularized liver scaffolds through the portal vein. We found that the scaffolds were easily recellularized with the GFP-labeled iHPCs [Fig. 3(A)]. In fact, the transduced iHPCs were able to survive and proliferate for up to 2 weeks in the 3-D culture [Fig. 3(A), panels a and d vs. b, c, e, and f]. H&E staining of the *in vitro* cultured scaffolds confirms that the perfused iHPCs survived and proliferated in the decellularized liver scaffolds. Thus, these *in vitro* findings suggest that

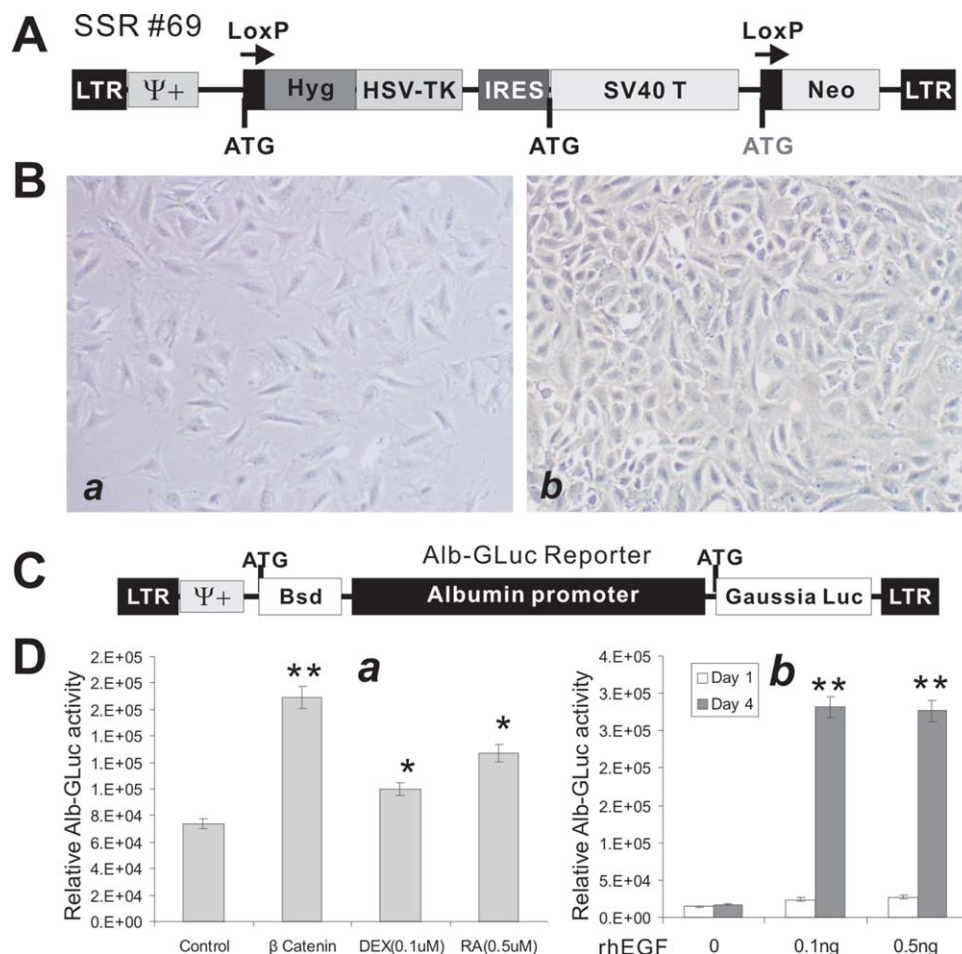


**FIGURE 2.** Establishment and characterization of immortalized mouse fetal hepatic progenitor cells (iHPCs). **A**, Schematic representation of the reversible immortalization retroviral vector SSR #69.<sup>26–28</sup> **B**, Growth and morphological features of the primary (a) and the immortalized HPCs (iHPCs; b). The immortalization was carried out as described.<sup>23,24</sup> The cells were seeded at the same density and were photographed at day 4 after plating. Representative images are shown. **C**, Construction of an albumin promoter-driven Gaussia luciferase reporter (Alb-GLuc). A 2.5-kb fragment containing the mouse albumin promoter region was cloned in front of Gaussia luciferase, resulting in the Alb-GLuc reporter, which was used to make stable Alb-GLuc reporter lines. **D**, The Alb-GLuc reporter is used to monitor the differentiation status of the iHPCs. Several known hepatic differentiation factors, including  $\beta$ -catenin, dexamethasone, and retinoic acid (a) and rhEGF (b), were shown to induce Alb-GLuc activities. \*,  $p$ -value < 0.05 and \*\*,  $p$ -value < 0.001. [Color figure can be viewed in the online issue, which is available at [wileyonlinelibrary.com](http://wileyonlinelibrary.com).]

the scaffolds may provide a suitable environment for iHPCs' survival and proliferation.

### The decellularized liver scaffolds provide biocompatible 3-D environment to support the proliferation and differentiation of iHPCs in a mouse renal capsule grafting model

We further tested the *in vivo* properties of the decellularized liver scaffolds in a mouse renal capsule implantation model. Subconfluent firefly luciferase-tagged iHPCs were first transduced with Ad-EGF or control AdGFP for 24 h [Fig. 4(A)], collected, and perfused into the decellularized liver scaffolds. The recellularized scaffolds were cultured for another 24 h and then gently cut into small pieces, and implanted into the left kidney capsule of athymic nude mice [Fig. 4(B)]. Scaffolds without recellularization were also performed as a negative control. The cell survival and proliferation of the implanted scaffolds was readily monitored by

whole body imaging. While the iHPCs were shown to survive in the implants for up to 10 days, EGF significantly promoted the survival and proliferation of the implanted iHPCs when compared with the GFP controls [Fig. 4(C)]. Nonetheless, there was a time point-dependent decrease in the signal intensities of Xenogen bioluminescence imaging analysis in EGF-stimulated iHPCs [Fig. 4(D)]. The decreased signal intensity may indicate that the iHPCs reached the maximum proliferation capacity in the scaffold environment or the iHPCs and/or the iHPCs were undergoing differentiation/maturation.

When the recellularized liver scaffold implants were retrieved and subjected to histologic and immunochemical analyses, we found that the iHPCs were able to proliferate in the scaffolds as indicated by the H&E staining [Fig. 5(A)]. Immunohistochemical staining using anti-GFP antibody indicated that most of the implanted iHPCs were transduced by adenoviral vectors [Fig. 5(B)]. We further examined the

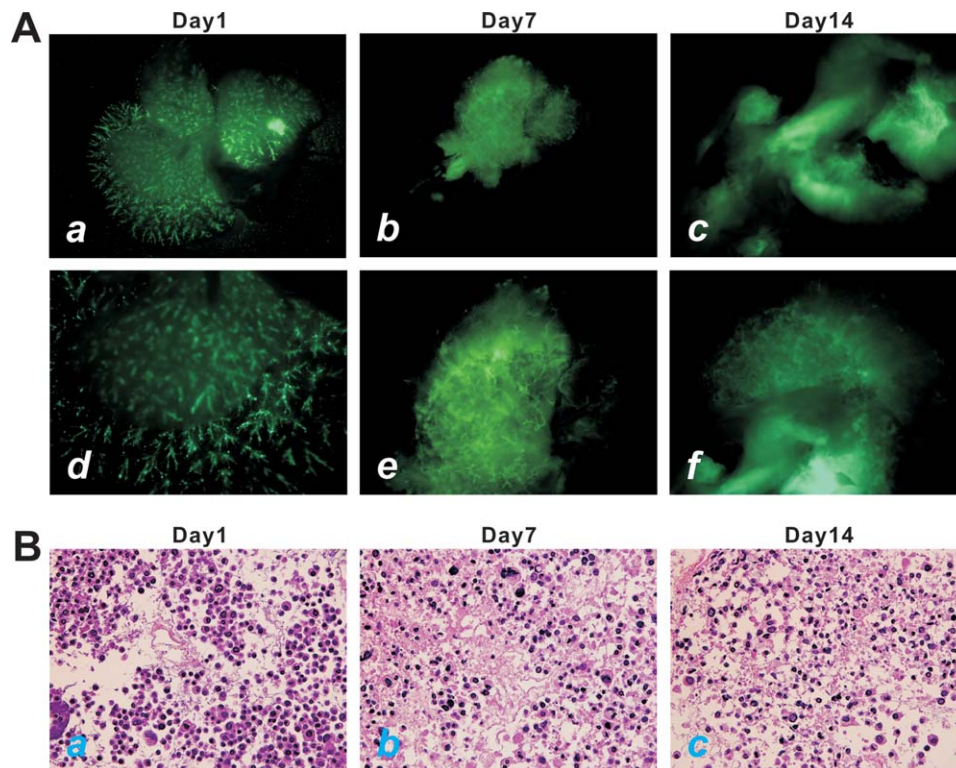


**FIGURE 3.** Decellularized liver scaffolds support iHPC proliferation in 3-D culture *in vitro*. A, Subconfluent iHPCs infected with AdGFP were perfused into the decellularized liver scaffolds (approximately  $10^{e7}$  cells/scaffold). GFP signal was detected at day 1 (a and d), day 7 (b and e), and day 14 (c and f). Panels a–c, lower magnification; panels d–f, higher magnification. B, H&E staining of the decellularized liver scaffolds seeded with iHPCs. The iHPC-seeded scaffolds were harvested at day 1 (a), day 7 (b), and day 14 (c), and frozen sectioned for H&E staining. Representative results are shown. [Color figure can be viewed in the online issue, which is available at [wileyonlinelibrary.com](http://wileyonlinelibrary.com).]

expression of the hepatocyte-specific marker albumin and found that the EGF-transduced iHPCs exhibit a higher level of albumin expression than that of the control GFP-treated cells [Fig. 5(C), panels c vs. b]. Interestingly, the recellularization of the biomaterial scaffolds was accompanied with vascularization within the scaffolds, as indicated by the immunostaining with the antibody against endothelial marker CD31 [Fig. 5(D), panels b and c vs. a]. Thus, these results strongly suggest that EGF-stimulated iHPC cells may proliferate and differentiate into mature hepatocytes in the decellularized liver scaffolds *in vivo*.

## DISCUSSION

Organ transplantation has been hampered by limited availabilities of quality organs. In the United States, it is estimated about 27,000 deaths annually are caused by liver diseases. Liver transplantation is the established treatment for individuals with acute liver failure, end-stage liver disease, or inherited liver-based metabolic disorders. Furthermore, the complexity liver functions make it impossible to use simple mechanical devices to provide temporary support. The scarcity of donor livers leads to too many patients on the waiting list, many of whom may never undergo liver transplantation. While orthotopic transplantation remains as an optimal option, the increasing donor organ shortage

requires consideration of alternative emerging technologies.<sup>2</sup> One such technology is to use cell transplantation.<sup>1–4,40</sup>

Here, we investigate if the decellularized liver matrix scaffolds can efficiently support the survival and proliferation of hepatic progenitor cells. Using a simplified portal vein perfusion procedure, we can effectively decellularize the mouse liver tissues, as assed by histologic examination and total DNA content determination. We further establish and characterize the reversibly iHPCs derived from mouse E13.5–E14.5 embryos. Through port vein perfusion, we are able to effectively recellularize the decellularized liver scaffolds. The perfused iHPCs can survive and proliferate in the 3-D scaffolds *in vitro*, as well as in a kidney capsule implantation model of athymic nude mice. Differentiation promoting factor EGF is shown to significantly promote the survival and differentiation of the implanted iHPCs. The recellularization of the biomaterial scaffolds is also accompanied with vascularization within the scaffolds. Thus, our results demonstrate that decellularized liver scaffolds may be ideal scaffolds for hepatocyte transplantation.

Numerous methods can be used to decellularize biologic organs, including physical, enzymatic and chemical.<sup>1–7</sup> In most cases, the detergent SDS followed by Triton X-100 is proven as an efficient method, which is also confirmed in our case. We have demonstrated that the decellularization can be effectively achieved acellular matrix within several

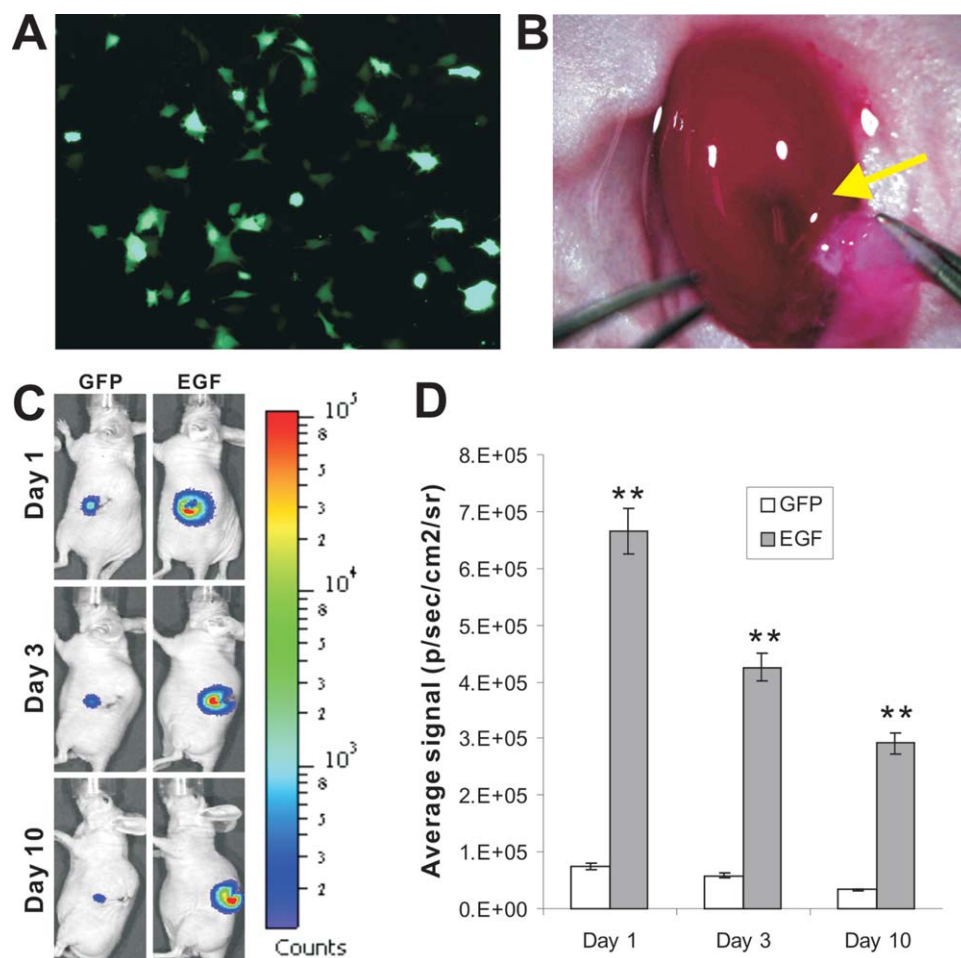


**FIGURE 4.** The iHPCs can survive and proliferate effectively in the decellularized liver scaffolds in the renal capsule grafting assays. A, The iHPCs were stably tagged with firefly luciferase (iHPC-FLuc) and infected with either AdGFP or Ad-EGF. The GFP expression was examined at 24h post-infection. A representative image from Ad-EGF infection is shown. B, The renal capsule grafting assay of the decellularized liver scaffolds seeded with iHPC-Luc cells. Approximately  $10^{27}$  iHPC-FLuc cells were transduced with AdGFP or Ad-EGF for 16 h, collected, and perfused into the decellularized liver scaffolds. Small pieces of the cell-loaded scaffolds were implanted into the left renal capsules of athymic nude mice (indicated by an arrow;  $n = 5$  per group). A representative image is shown. C and D, Monitoring the EGF-promoted cell proliferation in renal capsule using xenogen bioluminescence imaging analysis. At the indicated time points post rafting, the animals were subjected to the Xenogen IVIS 200 Imaging System (C). The average signal intensities were quantitatively calculated using Xenogen's Living Image software (D), as described previously.<sup>13,29,33</sup> \*\* indicates that  $p$ -values were  $<0.01$  when the average signals of the EGF-treated groups were compared with that of the GFP control groups'. [Color figure can be viewed in the online issue, which is available at [wileyonlinelibrary.com](http://wileyonlinelibrary.com).]

hours. The whole procedure can be performed at room temperature, although the sterility is required for the entire procedure.

Although embryonic stem cells or induced pluripotent stem cells may serve a good resource for stem cell-based transplantation and therapies, their availability and potentially hazardous biosafety profiles may hamper their eventual applications in clinical settings. In this study, we have established and characterized the reversibly immortalized hepatic progenitor cells from mouse fetal liver using a retroviral vector expressing SV40 large T antigen flanked with Cre/loxP sites.<sup>26</sup> We have demonstrated that the immortalization process is reversible (data now shown). More importantly, the immortalized hepatic progenitor cells retain the differentiation potential upon proper differentiation stimuli, such as Wnt signaling, Dex, retinoic acids, or EGF. Thus, the iHPCs may be used as an important tool to investigate liver

cell transplantation, as well as the basic research about molecular mechanisms behind hepatocyte proliferation and differentiation. Taken together, our results have demonstrated that the decellularized liver matrix can be used as cell-friendly biomaterial scaffolds for hepatic progenitor cell transplantation.

## CONCLUSIONS

The objective of this study was to evaluate whether the decellularized liver scaffolds can efficiently support the survival and proliferation of hepatic progenitor cells. We have shown that mouse liver tissues can be efficiently decellularized through a simplified portal vein perfusion procedure. We establish and characterize the reversibly iHPCs and are able to effectively recellularize the decellularized liver scaffolds. The perfused iHPCs can survive and proliferate in the

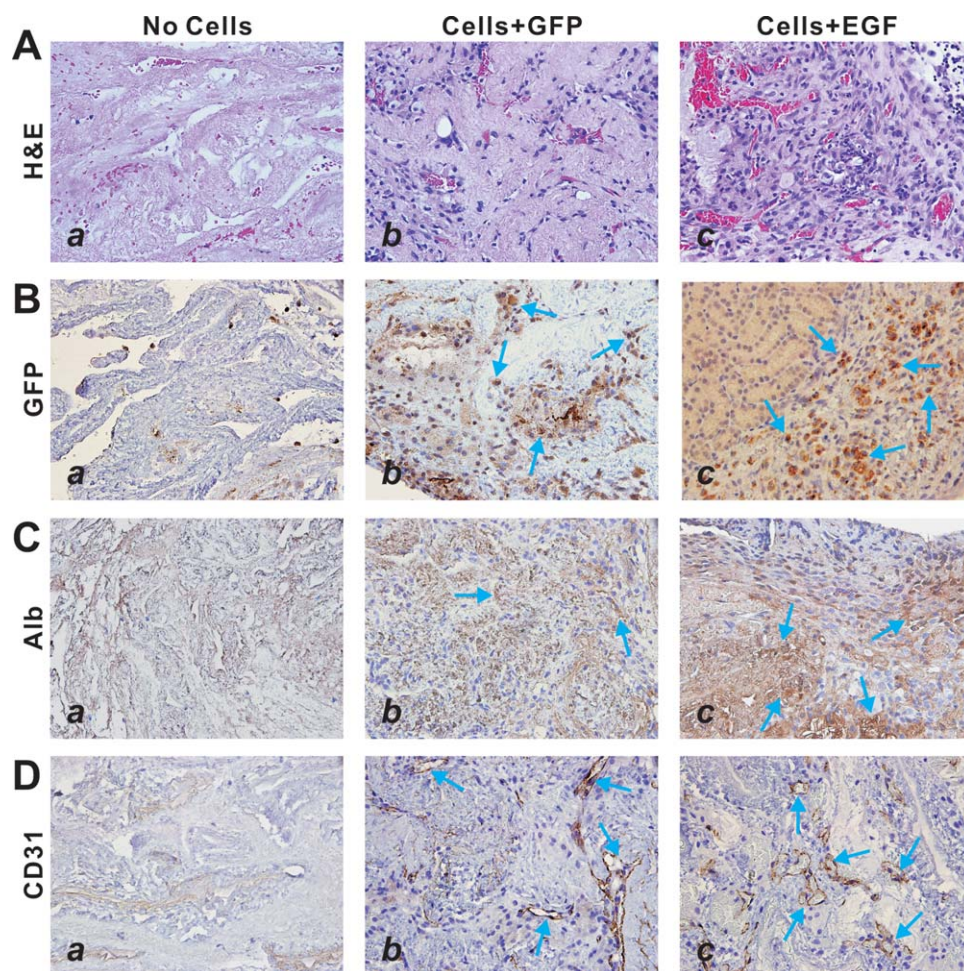


**FIGURE 5.** EGF-stimulated iHPC cells can proliferate and differentiate in the decellularized liver scaffolds *in vivo*. The renal capsule grafting samples were retrieved at 10 days postimplantation and subjected to frozen sectioning. The sections were subjected to H&E staining (A), anti-GFP immunohistochemical staining (B), antialbumin immunohistochemical staining (C), and anti-CD31 immunohistochemical staining (D). Control IgGs were used as negative controls (data not shown). Arrows indicate positive staining cells. Representative results are shown. [Color figure can be viewed in the online issue, which is available at [wileyonlinelibrary.com](http://wileyonlinelibrary.com).]

3-D scaffolds *in vitro* and in the kidney capsule implantation model of athymic nude mice. EGF is shown to significantly promote the survival and proliferation of the implanted iHPCs *in vivo*. The histologic and immunochemical analyses indicate that the iHPCs are able to proliferate and differentiate to mature hepatocytes upon EGF stimulation in the scaffolds. Therefore, our results demonstrate that decellularized liver scaffolds may effectively support the proliferation and differentiation of iHPCs, suggesting that the decellularized matrix may be used as ideal biocompatible scaffolds for hepatocyte transplantation.

#### ACKNOWLEDGMENT

The authors thank Dr. Philippe Leboulch of Harvard Medical School for the provision of SSR #69 vector.

#### REFERENCES

- Badylak SF, Taylor D, Uygun K. Whole-organ tissue engineering: Decellularization and recellularization of three-dimensional matrix scaffolds. *Annu Rev Biomed Eng* 2011;13:27–53.
- Fukumitsu K, Yagi H, Soto-Gutierrez A. Bioengineering in organ transplantation: Targeting the liver. *Transplant Proc* 2011;43: 2137–2138.
- Gilbert TW. Strategies for tissue and organ decellularization. *J Cell Biochem* 2012;113:2217–2222.
- Orlando G, Baptista P, Birchall M, De Coppi P, Farney A, Guimaraes-Souza NK, Opara E, Rogers J, Seliktar D, Shapira-Schweitzer K, Stratta RJ, Atala A, Wood KJ, Soker S. Regenerative medicine as applied to solid organ transplantation: Current status and future challenges. *Transpl Int* 2011;24:223–232.
- Song JJ, Ott HC. Organ engineering based on decellularized matrix scaffolds. *Trends Mol Med* 2011;17:424–432.
- Sullivan DC, Mirmalek-Sani SH, Deegan DB, Baptista PM, Aboushwareb T, Atala A, Yoo JJ. Decellularization methods of porcine kidneys for whole organ engineering using a high-throughput system. *Biomaterials* 2012;33:7756–7764.
- Traphagen S, Yelick PC. Reclaiming a natural beauty: Whole-organ engineering with natural extracellular materials. *Regen Med* 2009;4:747–758.
- Baptista PM, Siddiqui MM, Lozier G, Rodriguez SR, Atala A, Soker S. The use of whole organ decellularization for the generation of a vascularized liver organoid. *Hepatology* 2010;53: 604–617.

9. Brown B, Lindberg K, Reing J, Stolz DB, Badyrak SF. The basement membrane component of biologic scaffolds derived from extracellular matrix. *Tissue Eng* 2006;12:519–526.
10. Kang YZ, Wang Y, Gao Y. Decellularization technology application in whole liver reconstruct biological scaffold. *Zhonghua Yi Xue Za Zhi* 2009;89:1135–1138.
11. Shupe T, Williams M, Brown A, Willenberg B, Petersen BE. Method for the decellularization of intact rat liver. *Organogenesis* 2010;6:134–136.
12. Ott HC, Matthiesen TS, Goh SK, Black LD, Kren SM, Netoff TI, Taylor DA. Perfusion-decellularized matrix: Using nature's platform to engineer a bioartificial heart. *Nat Med* 2008;14:213–221.
13. Luo X, Chen J, Song WX, Tang N, Luo J, Deng ZL, Sharff KA, He G, Bi Y, He BC, Bennett E, Huang J, Kang Q, Jiang W, Su Y, Zhu GH, Yin H, He Y, Wang Y, Souris JS, Chen L, Zuo GW, Montag AG, Reid RR, Haydon RC, Luu HH, He TC. Osteogenic BMPs promote tumor growth of human osteosarcomas that harbor differentiation defects. *Lab Invest* 2008;88:1264–1277.
14. Tang N, Song WX, Luo J, Luo X, Chen J, Sharff KA, Bi Y, He BC, Huang JY, Zhu GH, Su YX, Jiang W, Tang M, He Y, Wang Y, Chen L, Zuo GW, Shen J, Pan X, Reid RR, Luu HH, Haydon RC, He TC. BMP9-induced osteogenic differentiation of mesenchymal progenitors requires functional canonical Wnt/beta-catenin signaling. *J Cell Mol Med* 2009;13:2448–2464.
15. Cheng H, Jiang W, Phillips FM, Haydon RC, Peng Y, Zhou L, Luu HH, An N, Breyer B, Vanichakarn P, Szatkowski JP, Park JY, He TC. Osteogenic activity of the fourteen types of human bone morphogenetic proteins (BMPs). *J Bone Joint Surg Am* 2003;85-A:1544–1552.
16. He TC, Zhou S, da Costa LT, Yu J, Kinzler KW, Vogelstein B. A simplified system for generating recombinant adenoviruses. *Proc Natl Acad Sci USA* 1998;95:2509–2514.
17. Kang Q, Song WX, Luo Q, Tang N, Luo J, Luo X, Chen J, Bi Y, He BC, Park JK, Jiang W, Tang Y, Huang J, Su Y, Zhu GH, He Y, Yin H, Hu Z, Wang Y, Chen L, Zuo GW, Pan X, Shen J, Vokes T, Reid RR, Haydon RC, Luu HH, He TC. A comprehensive analysis of the dual roles of BMPs in regulating adipogenic and osteogenic differentiation of mesenchymal progenitor cells. *Stem Cells Dev* 2009;18:545–559.
18. Kang Q, Sun MH, Cheng H, Peng Y, Montag AG, Deyrup AT, Jiang W, Luu HH, Luo J, Szatkowski JP, Vanichakarn P, Park JY, Li Y, Haydon RC, He TC. Characterization of the distinct orthotopic bone-forming activity of 14 BMPs using recombinant adenovirus-mediated gene delivery. *Gene Ther* 2004;11:1312–1320.
19. Luo J, Deng ZL, Luo X, Tang N, Song WX, Chen J, Sharff KA, Luu HH, Haydon RC, Kinzler KW, Vogelstein B, He TC. A protocol for rapid generation of recombinant adenoviruses using the AdEasy system. *Nat Protoc* 2007;2:1236–1247.
20. Peng Y, Kang Q, Luo Q, Jiang W, Si W, Liu BA, Luu HH, Park JK, Li X, Luo J, Montag AG, Haydon RC, He TC. Inhibitor of DNA binding/differentiation helix-loop-helix proteins mediate bone morphogenetic protein-induced osteoblast differentiation of mesenchymal stem cells. *J Biol Chem* 2004;279:32941–32949.
21. Luo Q, Kang Q, Si W, Jiang W, Park JK, Peng Y, Li X, Luu HH, Luo J, Montag AG, Haydon RC, He TC. Connective tissue growth factor (CTGF) is regulated by wnt and bone morphogenetic proteins signaling in osteoblast differentiation of mesenchymal stem cells. *J Biol Chem* 2004;279:55958–55968.
22. Sharff KA, Song WX, Luo X, Tang N, Luo J, Chen J, Bi Y, He BC, Huang J, Li X, Jiang W, Zhu GH, Su Y, He Y, Shen J, Wang Y, Chen L, Zuo GW, Liu B, Pan X, Reid RR, Luu HH, Haydon RC, He TC. Hey1 basic helix-loop-helix protein plays an important role in mediating BMP9-induced osteogenic differentiation of mesenchymal progenitor cells. *J Biol Chem* 2009;284:649–659.
23. Huang J, Bi Y, Zhu GH, He Y, Su Y, He BC, Wang Y, Kang Q, Chen L, Zuo GW, Luo Q, Shi Q, Zhang BQ, Huang A, Zhou L, Feng T, Luu HH, Haydon RC, He TC, Tang N. Retinoic acid signaling induces the differentiation of mouse fetal liver-derived hepatic progenitor cells. *Liver Int* 2009;29:1569–1581.
24. Bi Y, Huang J, He Y, Zhu GH, Su Y, He BC, Luo J, Wang Y, Kang Q, Luo Q, Chen L, Zuo GW, Jiang W, Liu B, Shi Q, Tang M, Zhang BQ, Weng Y, Huang A, Zhou L, Feng T, Luu HH, Haydon RC, He TC, Tang N. Wnt antagonist SFRP3 inhibits the differentiation of mouse hepatic progenitor cells. *J Cell Biochem* 2009;108:295–303.
25. Liu J, Ding X, Tang J, Cao Y, Hu P, Zhou F, Shan X, Cai X, Chen Q, Ling N, Zhang B, Bi Y, Chen K, Ren H, Huang A, He TC, Tang N. Enhancement of canonical Wnt/beta-catenin signaling activity by HCV core protein promotes cell growth of hepatocellular carcinoma cells. *PLoS One* 2011;6:e27496.
26. Westerman KA, LeBoulch P. Reversible immortalization of mammalian cells mediated by retroviral transfer and site-specific recombination. *Proc Natl Acad Sci U S A* 1996;93:8971–8976.
27. Yang K, Chen J, Jiang W, Huang E, Cui J, Kim SH, Hu N, Liu H, Zhang W, Li R, Chen X, Kong Y, Zhang J, Wang J, Wang L, Shen J, Luu HH, Haydon RC, Lian X, Yang T, He TC. Conditional immortalization establishes a repertoire of mouse melanocyte progenitors with distinct melanogenic differentiation potential. *J Invest Dermatol* 2012;132:2479–2483.
28. Huang E, Bi Y, Jiang W, Luo X, Yang K, Gao JL, Gao Y, Luo Q, Shi Q, Kim SH, Liu X, Li M, Hu N, Liu H, Cui J, Zhang W, Li R, Chen X, Shen J, Kong Y, Zhang J, Wang J, Luo J, He BC, Wang H, Reid RR, Luu HH, Haydon RC, Yang L, He TC. Conditionally immortalized mouse embryonic fibroblasts retain proliferative activity without compromising multipotent differentiation potential. *PLoS One* 2012;7:e32428.
29. He BC, Chen L, Zuo GW, Zhang W, Bi Y, Huang J, Wang Y, Jiang W, Luo Q, Shi Q, Zhang BQ, Liu B, Lei X, Luo J, Luo X, Wagner ER, Kim SH, He CJ, Hu Y, Shen J, Zhou Q, Rastegar F, Deng ZL, Luu HH, He TC, Haydon RC. Synergistic antitumor effect of the activated PPARgamma and retinoid receptors on human osteosarcoma. *Clin Cancer Res* 2010;16:2235–2245.
30. He BC, Gao JL, Luo X, Luo J, Shen J, Wang L, Zhou Q, Wang YT, Luu HH, Haydon RC, Wang CZ, Du W, Yuan CS, He TC, Zhang BQ. Ginsenoside Rg3 inhibits colorectal tumor growth through the down-regulation of Wnt/ss-catenin signaling. *Int J Oncol* 2011;38:437–445.
31. He BC, Gao JL, Zhang BQ, Luo Q, Shi Q, Kim SH, Huang E, Gao Y, Yang K, Wagner ER, Wang L, Tang N, Luo J, Liu X, Li M, Bi Y, Shen J, Luther G, Hu N, Zhou Q, Luu HH, Haydon RC, Zhao Y, He TC. Tetrandrine inhibits Wnt/beta-catenin signaling and suppresses tumor growth of human colorectal cancer. *Mol Pharmacol* 2011;79:211–219.
32. Rastegar F, Gao JL, Shenaq D, Luo Q, Shi Q, Kim SH, Jiang W, Wagner ER, Huang E, Gao Y, Shen J, Yang K, He BC, Chen L, Zuo GW, Luo J, Luo X, Bi Y, Liu X, Li M, Hu N, Wang L, Luther G, Luu HH, Haydon RC, He TC. Lysophosphatidic acid acyltransferase beta (LPAATbeta) promotes the tumor growth of human osteosarcoma. *PLoS One* 2010;5:e14182.
33. Su Y, Wagner ER, Luo Q, Huang J, Chen L, He BC, Zuo GW, Shi Q, Zhang BQ, Zhu G, Bi Y, Luo J, Luo X, Kim SH, Shen J, Rastegar F, Huang E, Gao Y, Gao JL, Yang K, Wietholt C, Li M, Qin J, Haydon RC, He TC, Luu HH. Insulin-like growth factor binding protein 5 suppresses tumor growth and metastasis of human osteosarcoma. *Oncogene* 2011;30:3907–3917.
34. Chen L, Jiang W, Huang J, He BC, Zuo GW, Zhang W, Luo Q, Shi Q, Zhang BQ, Wagner ER, Luo J, Wang M, Wietholt C, Luo X, Bi Y, Su Y, Liu B, Kim SH, He CJ, Hu Y, Shen J, Rastegar F, Huang E, Gao Y, Gao JL, Zhou JZ, Reid RR, Luu HH, Haydon RC, He TC, Deng ZL. Insulin-like growth factor 2 (IGF-2) potentiates BMP9-induced osteogenic differentiation and bone formation. *J Bone Miner Res* 2010;25:2447–2459.
35. Huang E, Zhu G, Jiang W, Yang K, Gao Y, Luo Q, Gao JL, Kim SH, Liu X, Li M, Shi Q, Hu N, Wang L, Liu H, Cui J, Zhang W, Li R, Chen X, Kong YH, Zhang J, Shen J, Bi Y, Statz J, He BC, Luo J, Wang H, Xiong F, Luu HH, Haydon RC, Yang L, He TC. Growth hormone synergizes with BMP9 in osteogenic differentiation by activating the JAK/STAT/IGF1 pathway in murine multilineage cells. *J Bone Miner Res* 2012;27:1566–1575.
36. Zhang W, Deng ZL, Chen L, Zuo GW, Luo Q, Shi Q, Zhang BQ, Wagner ER, Rastegar F, Kim SH, Jiang W, Shen J, Huang E, Gao Y, Gao JL, Zhou JZ, Luo J, Huang J, Luo X, Bi Y, Su Y, Yang K, Liu H, Luu HH, Haydon RC, He TC, He BC. Retinoic acids potentiate BMP9-induced osteogenic differentiation of mesenchymal progenitor cells. *PLoS One* 2010;5:e11917.

37. Hu N, Jiang D, Huang E, Liu X, Li R, Liang X, Kim SH, Chen X, Gao JL, Zhang H, Zhang W, Kong YH, Zhang J, Wang J, Shui W, Luo X, Liu B, Cui J, Rogers MR, Shen J, Zhao C, Wang N, Wu N, Luu HH, Haydon RC, He TC, Huang W. BMP9-regulated angiogenic signaling plays an important role in the osteogenic differentiation of mesenchymal progenitor cells. *J Cell Sci* 2013;126:532–541.
38. Haydon RC, Deyrup A, Ishikawa A, Heck R, Jiang W, Zhou L, Feng T, King D, Cheng H, Breyer B, Peabody T, Simon MA, Montag AG, He TC. Cytoplasmic and/or nuclear accumulation of the beta-catenin protein is a frequent event in human osteosarcoma. *Int J Cancer* 2002;102:338–342.
39. Haydon RC, Zhou L, Feng T, Breyer B, Cheng H, Jiang W, Ishikawa A, Peabody T, Montag A, Simon MA, He TC. Nuclear receptor agonists as potential differentiation therapy agents for human osteosarcoma. *Clin Cancer Res* 2002;8:1288–1294.
40. Zhou P, Lessa N, Estrada DC, Severson EB, Lingala S, Zern MA, Nolte JA, Wu J. Decellularized liver matrix as a carrier for the transplantation of human fetal and primary hepatocytes in mice. *Liver Transpl* 2011;17:418–427.